Using ^{36}Cl exposure dating to date mass movement and assess land stability on the Nicholas Range, Tasmania

Adrian J. Slee[1], Peter D. McIntosh[1], and Timothy T. Barrows[2]

[1] *Forest Practices Authority, 30 Patrick Street, Hobart, Australia, 7000*

[2] *Department of Geography, University of Exeter, EX4 4RJ United Kingdom*

ORCID (A Slee): 0000-0002-6299-3146

Acknowledgements

We thank Gareth Tempest (Forestry Tasmania) and Stephanie Mills for assistance during fieldwork. Funding for this project was provided by the Tasmanian Forest Practices Authority.

Abstract Detailed mapping of dolerite slope deposits overlying sedimentary Triassic rocks on the northern slopes of the Nicholas Range in north-eastern Tasmania has revealed an extensive mass movement complex. Landforms north of the summit plateau of the Nicholas Range include: (1) a cliff of dolerite columns with associated scree slopes at its base; (2) a topple landscape consisting of several topples that have fallen in a north-easterly direction; (3) a "ripple" landscape consisting of a series of long boulder ridges aligned approximately east-west. Exposure dating of three large boulders (collapsed dolerite columns) from a ridge within the ripple landscape gave a mean age of 52.1±1.9 ka using ^{36}Cl. This is the minimum age for collapse of the dated columns from the cliff face c. 750 m to the south. Boulder ages and landscape morphology indicate that the ripple landscape developed by physical and chemical degradation and concurrent northern displacement of topples over a slip plane formed at the contact between dolerite colluvium and underlying Triassic sedimentary rocks. There is no evidence of movement today, other than localised debris flows associated with knickpoints in streams, and it is deduced that movement on the slip plane occurred under a cooler climate than that prevailing today, possibly under the influence of melting of winter snow during the last glacial cycle. As there is no evidence of significant recent mass movement and forests in the area are likely to have experienced many stand-destroying forest fires in the Holocene, forest harvest is not considered to pose a risk to landscape stability.

Keywords Exposure dating, mass movement, dolerite terrain, topples, last glacial

Introduction

Dating of landslides using exposure dating has been found to be useful worldwide (Ballantyne and Stone 2004, Sewell et al. 2006, Panek 2015, Margirier et al. 2015, Sturzenegger et al. 2015). Panek (2015) pointed out that more research need to be done to date landslides in areas little affected by tectonic activity. In Australia only one landslide has been dated by exposure dating techniques: the South Sister landslide on the Nicholas Range in northeast Tasmania (McIntosh and Barrows, 2011). These authors used exposure dating with ^{36}Cl to determine that a landslide in dolerite terrain was 80–90 ka old (i.e. collapse occurred and landsliding began during the later stages of MIS 5). They suggested landslide initiation in cooler conditions than those currently prevailing, and that instability may have resulted from heavy snow accumulation in winter followed by spring snow melt, which would have saturated the contact between the dolerite colluvium and underlying subhorizontal Triassic strata.

This suggestion was supported by Slee et al. (2015) who presented geomorphic evidence for humid conditions along the Australian east coast during the last glacial cycle (defined as spanning MIS 5d-2, 109–14 ka (Liesiecki and Raymo 2005)) and by the work of McIntosh et al. (2012) who attributed a well-developed palaeosol dated to 21–16 ka in northeast Tasmania aeolian deposits to wet conditions in eastern Tasmania during the Last Glacial Maximum (LGM). These conclusions were supported by an increase in wet-favouring taxa in a depression on the Freycinet Peninsula in eastern Tasmania between 22 and 17 ka (Mackenzie 2010; Mackenzie and Moss 2014).

The presence on the north face of the Nicholas Range of dolerite topples, dolerite colluvium, debris mounds and large boulders several hundreds of metres from in-situ dolerite indicates extensive mass movement in dolerite colluvium, which is a widespread soil parent material in Tasmania (Green et al. 2012), and raises the question of whether forest operations on doleritic terrain might reactivate land instability. Further research on the landforms of the Nicholas Range were therefore conducted with the following aims: (1) to map and describe the landslides; (2) determine their age; (3) to infer the climatic conditions that influenced the formation of the mass-movement landscape; and (4) to determine the risk of present-day movement.

Site characteristics

The Nicholas Range (Fig. 1) is a 12 km long east-west ridge rising to 859 m asl at 41°32 S 148°06 E, 20 km from the coast of north-east Tasmania. The bedrock geology has been mapped by McClenaghan (2006). The range is capped by a horizontal Jurassic dolerite sill that forms a summit plateau averaging 820 m asl.

Surrounding the summit plateau cliffs up to 80 m high and steep scree slopes grade into gentler slopes mantled by dolerite colluvium overlying benches of subhorizontal Triassic strata composed of massive sandstone, mudstone and coal measures at approximately 560 m asl. The underlying sedimentary bedrock including Permian strata is exposed only in deep gullies, mostly below 500 m asl, which have been over-steepened by knick-point retreat and fluvial incision. In places dolerite colluvium and alluvium partly fills valleys to 200 m asl. The slope deposits of the Nicholas Range and dolerite terrain of eastern Tasmania broadly correspond with the stratigraphically controlled hill country mass-movement terrain described in New Zealand by Crozier (2010).

The study site (Fig. 2), extends north from the crest of the Nicholas range (820 m) to about 500 m altitude and covers 280 ha, but detailed observations were restricted to land lying between 780 m and 500 m asl on the upper northern slopes of the Nicholas Range. The area is forested and *Eucalyptus delegatensis* is the dominant species. It encompasses the hilly slopes immediately adjacent to steep scree slopes and cliff faces defining the edge of the summit plateau and the distal rolling slopes including the wide structural bench formed over Permo–Triassic strata.

The study area was selected for its unusual landforms, which include a series of doleritic boulder ridges and large isolated dolerite monoliths (displaced dolerite columns), a large enclosed depression, and a large rotational slump complex hosting boulder caves (Slee et al. 2011) immediately north of Mt Nicholas. The largest ridges are 1 km long and 50 m wide. They are aligned approximately east-west and are roughly parallel to each other, producing a "ripple" landscape (described in more detail below). Large dolerite boulders up to 8 m long and 3 m wide are clearly derived from columns visible in the dolerite cliffs on the Nicholas Range to the south. The boulders are most common on the northern (front) edges of ridges, where they are preferentially oriented with long axes north-south.

At present the east coast of Tasmania has a dry Mediterranean maritime climate with warm summers and mild winters. The mean maximum monthly temperature at Fingal at 237 m altitude 16 km southwest of the Nicholas Range is 17.8ºC and the mean monthly minimum temperature is 5.3ºC. During winter, inland frosts are common and infrequent snow can fall on the higher summits. Mean annual precipitation, recorded at the Cornwall weather station on the southern slopes of the Nicholas Range (41°56'S: 148°14'E; 338 m asl), is 1019 mm. (All data from Bureau of Meteorology 2017.) Rainfall is fairly constant throughout the year, however cut-off east coast low pressure systems producing heavy rainfall and precipitation exceeding 150 mm in 24 h are a feature of the region's climate.

Methods

Mapping

Landforms were mapped utilising satellite imagery and aerial photographs supplemented by extensive ground traverses using a Garmin GPS, in a similar fashion to the work of Van Eckhaut et al. (2005). The landform map was overlaid on a LIDAR-derived hill shade map (DPIPWE 2017) to generate Fig. 2.

Exposure dating

Three large boulders (NIC-01, 02 and 03), identified as collapsed and transported dolerite columns, now lying on on the northern side of a boulder ridge at 148°7'17E,: 41°32'16S were selected for sampling because of their large size (6–8 m long) (Figs 2 and 3). A total of five samples were collected (Table 1). Three samples labelled 'A' were collected from the upward-facing sides of the three columns. These were collected 5.5, 5.2 and 3.65 m respectively from the presumed tops (identified by their sub-rounded shape) of columns NIC-01, 02 and 03. Column NIC-03 was about 40 m east of boulders NIC-01 and 02. Two 'B' samples were collected from the rounded ends of columns NIC-01 and NIC-02 to determine whether the tops of columns had been exposed before column collapse, following the approach of Barrows et al. (2004). Both A and B samples were taken from massive unjointed surfaces showing no recent rock spalling. The column from which NIC-01 was sampled showed a plumose fracture pattern suggestive of stress release along a joint.

Sample preparation techniques are described by Barrows et al. (2002). Chemical data for the samples are presented in Table 2. The isotopic ratio of ^{36}Cl/Cl was measured by accelerator mass spectrometry on the 14UD accelerator at the Australian National University. Exposure ages were calculated using the conventional approach (Gosse and Phillips 2001). Production pathways for cosmogenic ^{36}Cl and production rates follow Barrows et al. (2002). Exposure ages were calculated using geographic latitude, without any erosion correction and include estimated ^{36}Cl production from Fe and Ti (Barrows et al. 2002).

The exposure ages for A samples are calculated on the basis of a simple exposure history with shielding only from the horizon (Table 3). If there has been a significant change in boulder orientation, a significant transport time, or soil cover since initial column collapse, these will be minimum ages. The exposure ages for the B samples in Table 3 are calculated using the horizon only. The shielding values included in Table 1 represent self-shielding by the block in the present orientation.

Results

Mapping and landform characterisation

Seven major landform units were mapped (Fig. 2): plateau, cliffs, topple landscape, ripple landscape, slumped ripple landscape, colluvial/alluvial slopes, and sedimentary bedrock (Fig. 2). Within the topple landscape, ripple landscape and slumped ripple landscape, topples, dolerite boulder ridges, isolated large boulders, springs, creeks, recent landslides and boulder caves were noted. The colluvial/alluvial slopes are dissected by deeply incised gullies.

In the west of the study area below Mt Nicholas, a very large topple (and associated landslide backwall) forms a ridge with the original structure of vertical fitting columns still evident, but now tilted to the northeast. This topple has similar morphology to topples described by Caine (1983, photographs 18 and 19) and Hungr et al. (2014). Extending 500 m northeast of the most recent topple are the remains of at least two other topples. The topples have formed a prominent embayment in the dolerite cliff (Fig. 2), approximately 400 m wide and extending 500 m downslope from the cliff.

Although the most recent topple ridge retains columnar structure, the older (northern) topples in the topple landscape have the form of chaotic boulder ridges. The largest boulders are up to 25 m long, and the northeastern ridge contains a boulder cave with passages up to 35 m long and chambers 6 m high. The cave appears to have formed by disintegration of the columnar structure of the original topple, either by the effect of freeze/thaw, or by the effect of mass movement induced by the pressure of the subsequent topples upslope, or both processes. Present stability within the cave is indicated by the rare coralline carbonate growths on the lower surfaces of some boulders (Slee et al. 2011), but minor rock breakdown is evidenced by fresh dolerite rubble in the cave floor.

North of the topple landscape (in the west), and north of the cliff face of the Nicholas Range (in the east) the "ripple" landscape consists of subdued ridges up to 1 km long and 50 m wide, aligned approximately east-west and roughly parallel to each other. Large dolerite boulders in these subdued ridges are up to 8 m long and 3 m wide and are clearly displaced columns similar to those visible in the dolerite cliffs on the Nicholas Range to the south. The boulders are most common on the northern (front) edges of ridges, where they are preferentially oriented with long axes aligned approximately north-south. Ridges are separated by depressions, some of which contain fine clayey sediments. In the northern part of the ripple landscape slumping has occurred. The largest slump is 550 m wide from east to west and 350 m wide north to south.

North of the ripple landscape is a gullied landscape formed by stream erosion of the underlying sub-horizontal Permo-Triassic sedimentary rocks. The streams originate at the numerous seepages which occur at the contact of the dolerite colluvium and the underlying impermeable sedimentary strata.

Exposure ages

The A samples range in age from 51–70 ka (Table 3 and Fig. 4). Ages for NIC-02A and 03A are statistically identical, but the age for NIC-01A is ~20 ka older. The B samples both have ^{36}Cl concentrations higher than expected based on the column side ages. If the blocks have remained in their same geometry for the entire length of exposure time recorded by the NIC-01A and 02B samples, then the top of the blocks are the equivalent of 22 and 10 ka older respectively. However, these are not real differences in age and indicate that there was a brief earlier period of exposure for each of the blocks, probably at the Mt Nicholas cliff face before the topple. The nearby South Sister landslide was much closer to its source where there is no cliff and the blocks dated there were unlikely to have been exposed before mass movement. In contrast, on Mt Wellington in southern Tasmania, column ends and column sides show a much higher discrepancy between exposure ages (Barrows et al. 2004) indicating long exposure of tops of columns before toppling.

The simplest explanation for the Mt Nicholas ages is that the columns were exposed in an episode of toppling at 52.1 ± 1.9 ka (i.e. in MIS 3 57-29 ka (Liesiecki and Raymo 2005)), the weighted mean of the two youngest samples. Given the inheritance on the upper ends of the columns, it is likely sample NIC-01A was exposed at the free face. Its greater age matches the approximate age difference of the end of the NIC-02 column.

Discussion and conclusions

Landforms and landform development

Caine (1983) developed ideas to explain toppling and topple movement in both glaciated and non-glacial doleritic landscapes in northeast Tasmania. Although Caine's work was mostly at higher altitude than Mt Nicholas, many of his observations and the processes he described apply to the study area. At Ben Lomond, Caine (1983) noted that high cliffs are generally stable under the present climate and that toppling probably occurred in the last glacial cycle. For cliff tops at about 1440 m altitude, he calculated a cliff retreat of 20 m

over the last 80 000 years. This can be regarded as a maximum average rate of retreat for the lower-altitude cliffs of the Nicholas Range, which would have been subjected to less marked climatic extremes than Ben Lomond. Relevant to processes on Mt Nicholas is Caine's observation (Caine 1983, p. 95) that some topples had moved far from their source, notably on the southern slopes of Mt Victoria where, as at Mt Nicholas, dolerite colluvium is underlain by sedimentary rocks. He also noted that the weight of 100 m of dolerite will produce a stress on underlying sediments approximately equivalent to the bearing capacity of siltstones and mudstones, and exceeding the bearing capacity of these rocks if they are saturated. Thus a steep cliff of dolerite resting on saturated sedimentary rocks will only remain intact if it is buttressed by deep colluvium. If the colluvium moves downslope (for example, as a landslide on a saturated slip plane), the steep cliff face will fail and a topple will result.

We suggest that the topple landscape on the northern slopes of Mt Nicholas, the ripple landscape and the slumped ripple landscape are three components of one overall process: mass wasting and downslope movement of cliff debris derived from columnar dolerite mountains under a colder climate than at present. We suggest the following model to explain these landforms. During the last glacial cycle mass wasting of the very steep cliff faces by toppling occurred intermittently. Each topple exerted a force on older topple debris further down slope, inducing it to slip over the contact with Triassic rocks below. In the cold climate episodes of the last glacial cycle such slippage would have been aided by saturation of the dolerite colluvium/Triassic contact by seasonal melting of thick winter snow cover, as suggested by McIntosh and Barrows (2011) for bouldery landslide deposits on slopes at nearby South Sister. In this way, the recognisable topples in the topple landscape unit have moved up to 750 m from the cliff face from which they are derived.

We note that Caine (1983, Fig. 5.7) described topples at distances up to 300 m from cliffs which had disintegrated into "ridges in talus". We suggest that the ripple landscape on the northern slopes of Mt Nicholas has formed by a similar process of topple disintegration and is the distal and older expression of the topple landscape. As the topples slowly moved northwards, many boulders within topples have broken up under the combined effects of physical weathering along joints and chemical weathering, the latter accentuated by burial of boulders in the acidic doleritic soils (Laffan et al. 1995, p. 155). However, the most massive and least jointed columns that were not buried in soils have survived in the older subdued topple landforms, which now take the form of low ridges. As in solifluction deposits (restricted to altitudes above 800 m (Caine 1983, p.20)), the forward slopes (risers) of the ripples are steeper than the back slopes (treads) because the advancing deposits are

attempting to override colluvium downslope. Close to the gullied alluvial landscape in sedimentary rocks the restraining effect of colluvium downslope is absent and recent slumping has resulted.

The coarse debris cascade from the Nicholas Range continues at present. One small rockfall/rockslide originating from the cliff exposed in the back-wall of the most recent topple was observed in November 2010.) Rockfalls and topples are likely to have been more frequent during the cold conditions of the last glacial cycle.

Exposures in road cuttings indicate that in the southern parts of the ripple landscape the 0–0.5 m surface layer is composed of angular and subangular dolerite cobble/boulder deposits (Fig. 5) with weakly weathered clasts having thin weathering rinds. These extremely stony deposits overlie strongly weathered (clayey) deposits containing occasional clasts that have developed thick weathering rinds. A veneer of angular stones and boulders over more clayey deposits is widespread in dolerite colluvium in Tasmania and attributed to freeze-thaw processes late in the last glacial cycle (McIntosh et al. 2012). The underlying weathered deposits are clearly much older and elsewhere (McIntosh et al. 2012, sites 48 and 49) similar clayey stony dolerite colluvium has been radiocarbon dated >45 ka. Close to the cliff the angular surface veneer is likely to be the distal component of screes formed by frost shattering of exposed rock on the cliff itself, but further away the boulders and debris of the topples will have been the local source.

Landslide classification and risk

With some variation in terminology to account for weathering processes, the landslides within the seven landscape units mapped can be classified using the Australian Geomechanics Society system (AGS 2007). The final phase of toppling must have happened very rapidly. Hence the near-source landslides in the topple landscape (Fig. 2) are classified as ‘Very Rapid Rock Topples’. A rock fall was experienced during this study so the risk of small-scale rock falls and topples is assessed as high.

In the discussion above we deduced that the ripple landscape is a result of physical and chemical weathering and displacement of topples that originally formed upslope. Technically the AGS classification requires displaced material to be described on the basis on what it was like before it was displaced (AGS 2007, p. 87) and does not take account of weathering since displacement. For the distal Mt Nicholas deposits which originated as rock topples it is more useful to describe the mass-movement material as debris (20%–80% of the particles larger than 2 mm and the remainder less than 2 mm) rather than rock. The type of movement which has displaced the ridges in the ripple landscape is not readily classified using the AGS scheme, although the ripple landscape (Fig. 2) bears comparison to landforms formed by debris creep, and the slumped ripple landscape to

landforms formed by debris lateral spread (AGS 2007, Fig. B1). There is no evidence, in the form of curved trees or tension cracks in the ground, of active movement at present, so the present rate of movement is assumed to be extremely slow (<15 mm per year in the AGS classification). If the modest rate of cliff retreat (20 m in 80 ka) calculated by Caine (1983) is accepted as a maximum for the lower-altitude Mt Nicholas cliff, then the dated boulders have moved about 730 m northwards in 52 ka, giving an average rate of movement of 14 mm per year. However, if the snow melt hypothesis discussed above is correct, rates of movement will have been faster in periods of cooler climate than at present, and conversely, less than 14 mm per year under the present climate regime, and possibly close to zero.

While forestry activity has been linked with the promotion of unstable slopes particularly within the first 1–10 years after harvest, due to root strength decline and subsequent soil binding decay (Montgomery et al. 2000; Imaizumi et al. 2008), no large-scale slope instability has been noted on the northern slopes of the range where harvest operations have occurred in the recent past. In addition, as the forested slopes of Mt Nicholas are likely to have experienced numerous vegetation-destroying wildfires in the Holocene, without obvious effects on land stability, forest harvest conforming to strict environmental guidelines (Forest Practices Authority 2015) on the slopes described and on similar landforms elsewhere is considered unlikely to induce or reactivate mass movement.

References

AGS 2007. Practice note guidelines for landslide risk management. *Australian Geomechanics* 42: 87–92.

Ballantyne CK, Stone JO (2004) The Beinn Alligin rock avalanche, NW Scotland: cosmogenic 10Be dating, interpretation and significance. *The Holocene* 14: 448-453

Barrows TT, Stone JO, Fifield LK, Cresswell RG (2002) The timing of the Last Glacial Maximum in Australia. *Quaternary Science Reviews* 21: 159-173

Barrows TT, Stone JO, Fifield LK (2004) Exposure ages for Pleistocene periglacial deposits in Australia. *Quaternary Science Reviews* 23: 697–708

Bureau of Meteorology (2007) Climate Data Online. http://www.bom.gov.au/climate/data.

Caine N (1983) The Mountains of Northeastern Tasmania. Balkema, Rotterdam.

Crozier MJ (2010) Landslide geomorphology: An argument for recognition, with examples from New Zealand. *Geomorphology* 120: 3-15

DPIPWE (2007) The List Tasmania. http://maps.thelist.tas.gov.au/listmap/app/list/map

Forest Practices Authority (2015) Forest Practices Code. Forest Practices Authority, Hobart.

Gosse JC and Phillips FM (2001) Terrestrial in situ cosmogenic nuclides: theory and application. *Quaternary Science Reviews* 20: 1475–1560

Green DC, Brown AV, Calver CR, Corbett KD, Everard JL, Forsyth SM, Green G, Goscombe BD, Woolward I, Clark MJ, McClenaghan MP, Vicary M, Pemberton J, Seymour DB, Worthing M (1997) Geology of Tasmania 1:500 000. Mineral Resources Tasmania, Hobart.

Guzzetti F, Peruccacc S, Rossi M, Stark CP (2008) The rainfall intensity-duration control of shallow landslides and debris flows: an update. *Landslides* 5: 3-17

Hungr O, Leroueil S, Picarelli L (2014) The Varnes classification of landslide types, an update. *Landslides* 11: 167–194.

Imaizumi F, Sidle RC, Kamei R (2007) Effects of forest harvesting on the occurrence of landslides and debris flows in steep terrain of central Japan. *Earth Surface Processes and Landforms* 33: 827-840

Laffan M, Grant J, Hill R (1995) Soils of Tasmanian State Forests. 1. Pipers Sheet. Soils Bulletin No. 1. Forestry Tasmania, Hobart.

Lebourg T, Zerathe S, Fabre R, Giuliano J, Vidal M (2014) A Late Holocene deep-seated landslide in the northern French Pyrenees. *Geomorphology* 208: 1-10

Lisiecki LE, Raymo ME (2005) A Pliocene-Pleistocene stack of 57 globally distributed benthic D18O records. *Paleooceanography* 20, PA1003, doi:10.1029/2004PA001071, 17 p.

Mackenzie L (2010) Late Quaternary environments of Freycinet Peninsula, Eastern Tasmania. Honours Thesis, University of Queensland.

Mackenzie L, Moss P (2014) A late Quaternary record of vegetation and climate change from Hazards Lagoon, eastern Tasmania. *Quaternary International* (2014), http://dx.doi.org/10.1016/j.quaint.2014.11.051

Margirier A, Audin L, Carcaillet J, Schwartz S, Benavente C (2015) Tectonic and climatic controls on the Chuquibamba landslide (western Andes, southern Peru). *Earth Surface Dynamics* 3: 281-289

McClenagan MP (2006) Digital Geological Atlas 1:25000 series. Sheet 5840, Dublin Town. Mineral Resources Tasmania.

McIntosh PD, Barrows TT (2011) Morphology and age of boulder landslide deposits in forested terrain, Nicholas Range, Tasmania. *Zeitschift für Geomorphologie* 55: 383–393.

McIntosh PD, Eberhard R, Slee A, Moss P, Price DM, Donaldson P, Doyle R, Martins J (2012) Late Quaternary extraglacial cold-climate deposits in low and mid-altitude Tasmania and their climatic implications. *Geomorphology* 179: 21—39.

Montgomery DR, Schmidt KM, Greenberg HM, Dietrich WE (2000) Forest clearing and regional landsliding. *Geology* 28: 311-314

Panek T (2015) Recent progress in landslide dating: a global overview. *Progress in Physical Geology* 39: 168–198.

Sewell RJ, Barrows TT, Campbell SDG, Fifield LK (2006). Exposure dating (^{10}Be, ^{26}Al) of natural terrain landslides in Hong Kong, China, Special Paper of the Geological Society of America, pp. 131-146.

Slee A, McIntosh PD, Tempest G (2011) Boulder Caves of Mt Nicholas. *Caves Australia* (186).

Slee A, Shulmeister J (2015) The distribution and climatic implications of periglacial landforms in eastern Australia. *Journal of Quaternary Science*, *30*: 848-858. doi:10.1002/jqs.2823

Sturzenegger M, Stead D, Gosse J, Ward B., Froese C (2015) Palliser Rockslide based on ^{36}Cl terrestrial cosmogenic nuclide dating and debris volume estimations. *Landslides* 12: 1097-1106

Van Eckhaut MV, Poesen J, Verstraeten G, Vanacker V, Moeyersons J, Nyssen J, van Beek LPH (2005) The effectiveness of hillshade maps and expert knowledge in mapping old deep-seated landslides. *Geomorphology* 67: 351-363.

Fig. 1 Location map. Inset shows Tasmania. Map grid is GDA 1994 MGA Zone 55.

Fig. 2 The seven landscapes present within the study area interpreted from field work and remote mapping. Map grid is GDA 1994 MGA Zone 55.

Fig. 3 Landform map of the study area overlaid on LIDAR imagery. Map grid is GDA 1994 MGA Zone 55.

Fig. 4 Photographs of the three sites at which dolerite boulders were sampled for ^{36}Cl exposure dating. All photographs are taken facing approximately east; the boulders are aligned approximately north-south on the northern edges of boulder 'fronts' that form the ripple landscape described in the text. Ages obtained are shown.

Fig. 5 Weakly weathered angular and sub-angular dolerite boulders and cobbles form a veneer over older strongly weathered clay-rich dolerite deposits within the ripple landscape. The pick axe is 900 mm long.

Fig. 1

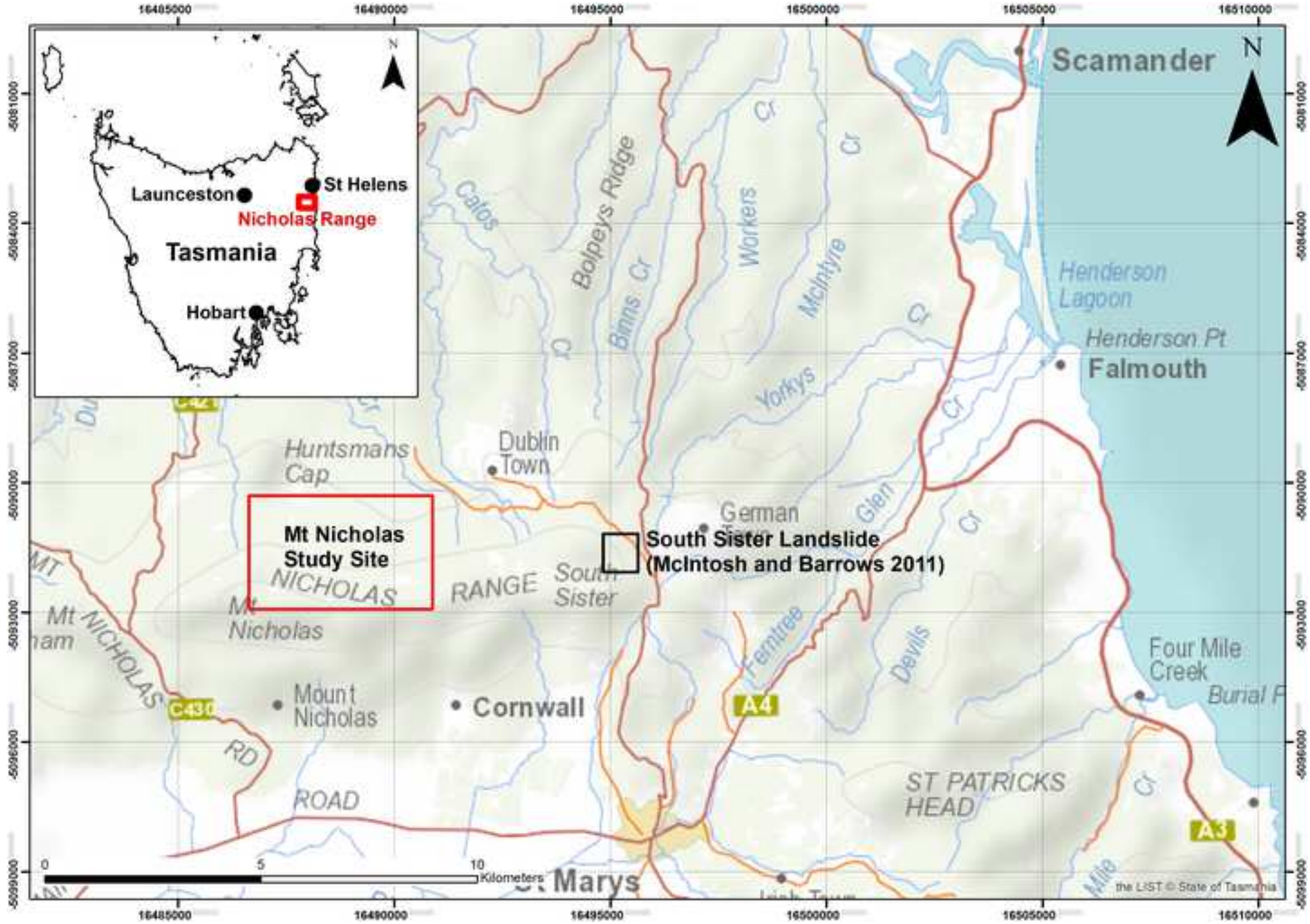
Launceston
St Helens
Nicholas Range
Tasmania
Hobart
Scamander
Henderson Lagoon
Henderson Pt
Falmouth
Bolpeys Ridge
Binns Cr
Workers Cr
McIntyre Cr
Yorkys Cr
Glen Cr
Devils Cr
Femtree
Huntsmans Cap
Dublin Town
German
South Sister
Mt Nicholas Study Site
South Sister Landslide (McIntosh and Barrows 2011)
NICHOLAS RANGE
Mt Nicholas
Mount Nicholas
Cornwall
C430
A4
A3
RD
ROAD
ST PATRICKS HEAD
Four Mile Creek
St Marys
0
5
10
Kilometers
the LIST © State of Tasmania
16485000
16490000
16495000
16500000
16505000
16510000
5081000
5084000
5087000
5090000
5093000
5096000
5099000

Fig. 2

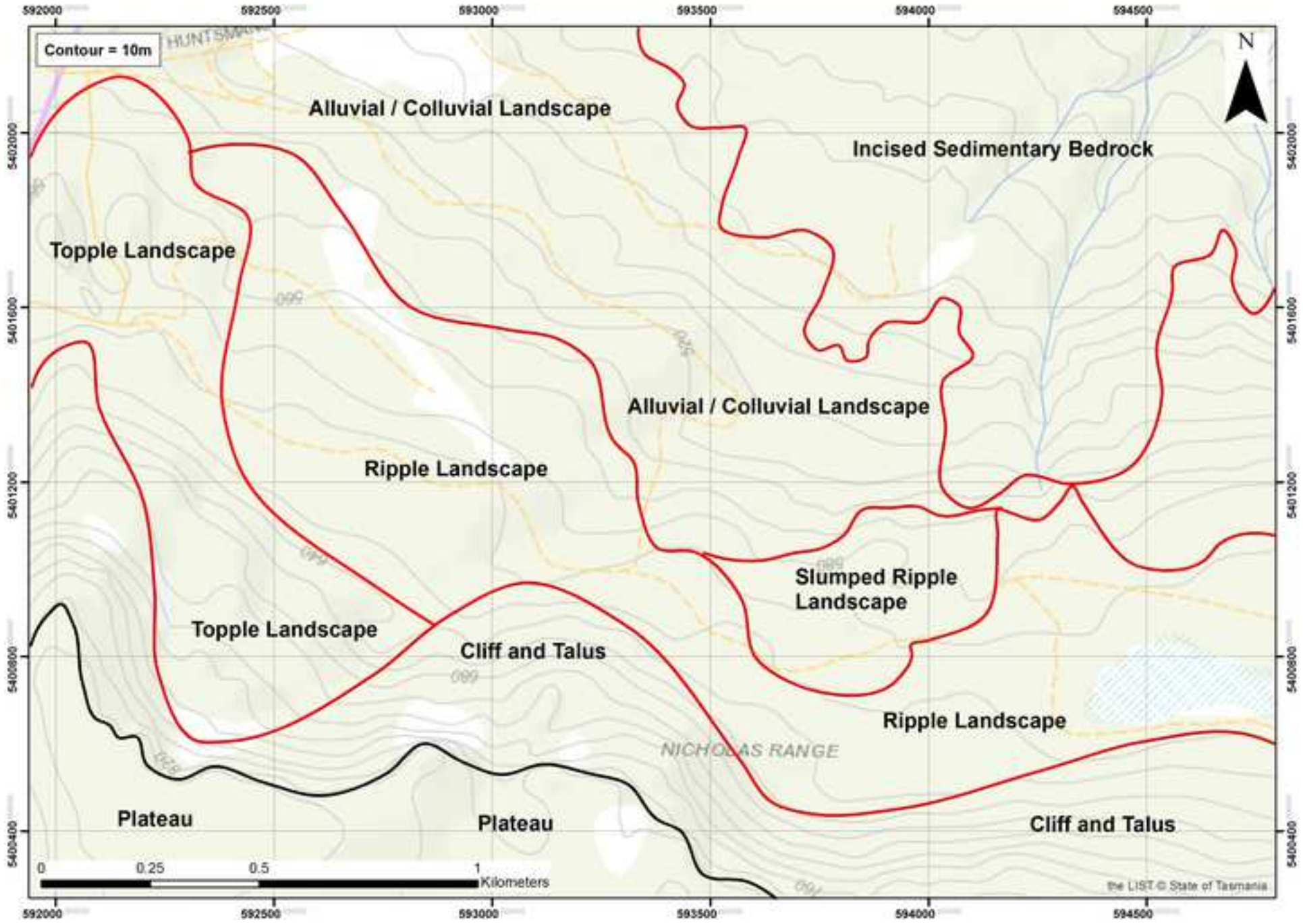
Contour = 10m
N
Alluvial / Colluvial Landscape
Incised Sedimentary Bedrock
Topple Landscape
Alluvial / Colluvial Landscape
Ripple Landscape
Slumped Ripple Landscape
Topple Landscape
Cliff and Talus
Ripple Landscape
NICHOLAS RANGE
Plateau
Plateau
Cliff and Talus
0
0.25
0.5
1
Kilometers
the LIST © State of Tasmania
592000
592500
593000
593500
594000
594500
5402000
5401600
5401200
5400800
5400400

Fig. 3

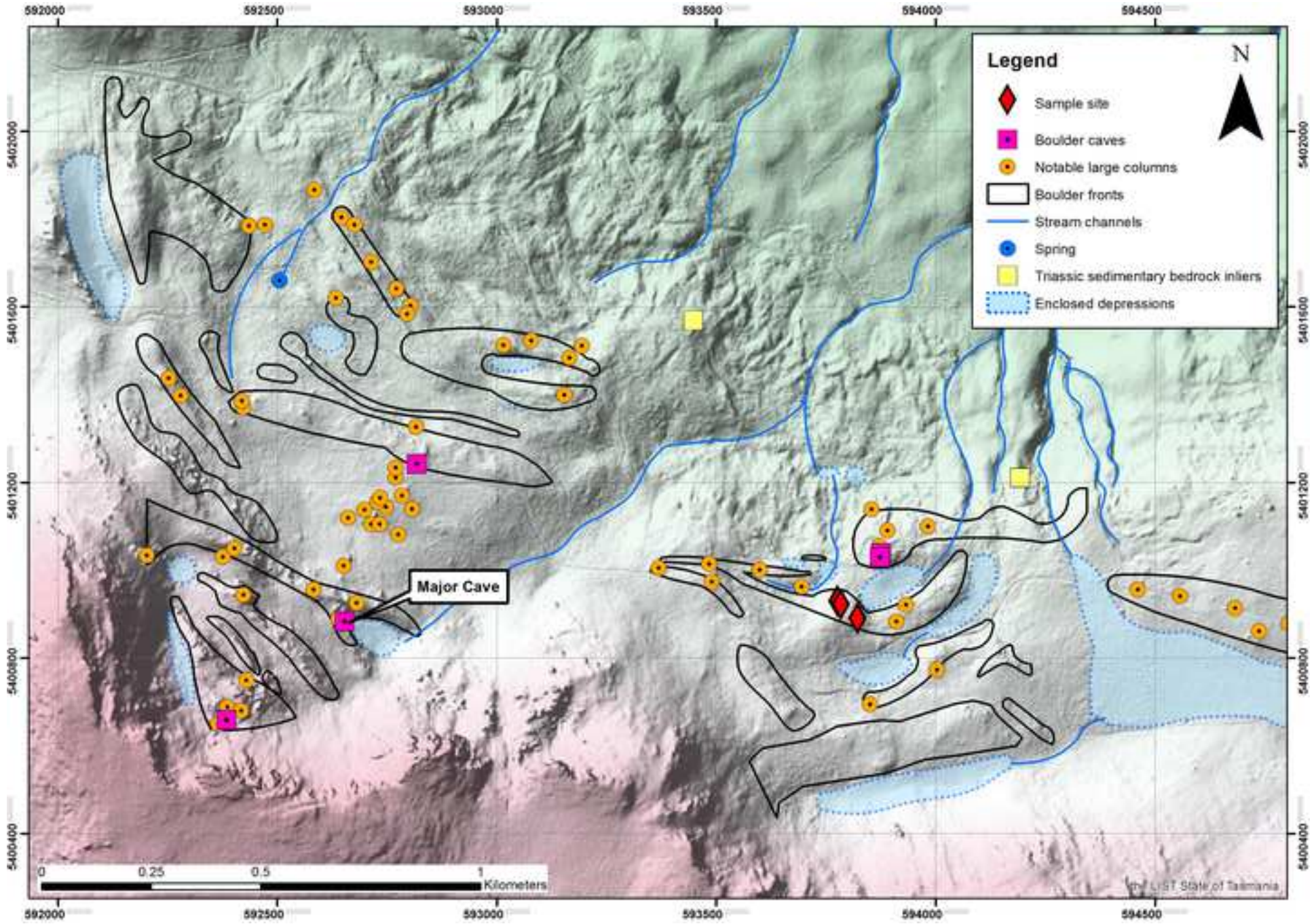
592000
592500
593000
593500
594000
594500
5402000
5401600
5401200
5400800
5400400
Legend
N
Sample site
Boulder caves
Notable large columns
Boulder fronts
Stream channels
Spring
Triassic sedimentary bedrock inliers
Enclosed depressions
Major Cave
0
0.25
0.5
1
Kilometers
© LIST State of Tasmania

Fig. 4

Fig. 5

Table 1 Site data.

Sample	Longitude (°E)	Latitude (°N)	Altitude (GPS) (m)	Lithology[1]	Shielding correction[2]	Thickness (cm)[3]
NIC-01A	148.12418	41.53779	622	dolerite		1.9
NIC-01B	148.12418	41.53779	622	dolerite	0.7698	2.8
NIC-02A	148.12432	41.5379	624	dolerite		4.6
NIC-02B	148.12432	41.5379	624	dolerite	0.8698	1.5
NIC-03A	148.12473	41.53815	623	dolerite		2.2

□□□dolerite □ = 2.7 g.cm^{-3}
2. Self-shielding; Site horizon correction = 0.9978 (included for NIC-01B and NIC-02B)
3. □ = 160 g.cm^{-2}

Table 2 Chemical analyses.

Target element data

Sample	K_2O (wt%)	CaO (wt%)	TiO_2 (wt%)	Fe_2O_3 (wt%)	Cl (ppm)
NIC-01A	0.99 ± 0.04	8.56 ± 0.08	0.7 ± 0.16	12 ± 0.18	13.22 ± 0.31
NIC-01B	0.95 ± 0.04	8.61 ± 0.08	0.75 ± 0.17	11.57 ± 0.17	21.94 ± 0.49
NIC-02A	0.96 ± 0.04	8.69 ± 0.08	0.71 ± 0.16	11.49 ± 0.17	4.36 ± 0.15
NIC-02B	0.88 ± 0.03	8.9 ± 0.08	0.71 ± 0.16	12.49 ± 0.19	8.02 ± 0.21
NIC-03A	0.85 ± 0.03	9.03 ± 0.08	0.76 ± 0.17	12.8 ± 0.19	5.96 ± 0.18

Trace element data

Sample	B[1] (ppm)	Sm (ppm)	Gd (ppm)	Th (ppm)	U (ppm)
NIC-01A	3 ± 1	3.26 ± 0.110	3.53 ± 0.210	3.34 ± 0.106	1.05 ± 0.097
NIC-01B	3 ± 1	3.37 ± 0.011	3.76 ± 0.033	2.53 ± 0.077	0.93 ± 0.019
NIC-02A	3 ± 1	2.94 ± 0.010	3.31 ± 0.023	2.84 ± 0.087	0.85 ± 0.018
NIC-02B	3 ± 1	2.66 ± 0.013	2.97 ± 0.026	2.98 ± 0.098	0.77 ± 0.017
NIC-03A	3 ± 1	3.10 ± 0.006	3.46 ± 0.023	3.03 ± 0.092	0.82 ± 0.018

[1]B estimated from Barrows *et al.* (2002) and McIntosh and Barrows (2011).

Table 3 Exposure ages[1].

Sample	Lab code	$[^{36}Cl]_c$ ($\times 10^4$ g^{-1})[2]	$[^{36}Cl]_r$ ($\times 10^3$ g^{-1})[3]	Exposure age (ka)
NIC-01A	ANU-C237-18	59.74 ± 2.35	1.61 ± 0.083	69.7 ± 3.6
NIC-01B	ANU-C237-15	60.63 ± 2.32	2.20 ± 0.088	<67.4 ± 3.5
NIC-02A	ANU-C237-20	43.24 ± 1.76	0.447 ± 0.021	53.4 ± 2.8
NIC-02B	ANU-C237-16	51.95 ± 2.10	0.440 ± 0.020	<63.5 ± 3.3
NIC-03A	ANU-C237-17	42.15 ± 1.72	0.444 ± 0.020	50.9 ± 2.6

[1]Data are normalised to the GEC standard ($^{36}Cl/Cl = 444 \times 10^{-15}$). Carrier $^{36}Cl/Cl = 1 \times 10^{-15}$. ^{36}Cl decay constant 2.3×10^{-6} yr^{-1}.
[2] c = cosmogenic component
[3] r = background nucleogenic component